

# ChemComm

Accepted Manuscript



This is an *Accepted Manuscript*, which has been through the Royal Society of Chemistry peer review process and has been accepted for publication.

*Accepted Manuscripts* are published online shortly after acceptance, before technical editing, formatting and proof reading. Using this free service, authors can make their results available to the community, in citable form, before we publish the edited article. We will replace this *Accepted Manuscript* with the edited and formatted *Advance Article* as soon as it is available.

You can find more information about *Accepted Manuscripts* in the [Information for Authors](#).

Please note that technical editing may introduce minor changes to the text and/or graphics, which may alter content. The journal's standard [Terms & Conditions](#) and the [Ethical guidelines](#) still apply. In no event shall the Royal Society of Chemistry be held responsible for any errors or omissions in this *Accepted Manuscript* or any consequences arising from the use of any information it contains.

# Supercharged Green Fluorescent Proteins as Bimodal Reporter Genes for CEST MRI and Optical Imaging

Cite this: DOI: 10.1039/x0xx00000x

A.Bar-Shir<sup>a,b</sup>, Y. Liang<sup>a,b</sup>, K.W.Y. Chan<sup>a,b</sup>, A.A. Gilad<sup>a,b,f</sup> and J. W. M. Bulte<sup>a-f</sup>

Received 00th January 2015,

Accepted 00th January 2015

DOI: 10.1039/x0xx00000x

www.rsc.org/

**Superpositively charged mutants of green fluorescent protein (GFP) demonstrated a dramatically improved chemical exchange saturation transfer (CEST) MRI contrast compared to their wild type counterparts. The mutants +36 GFP and +48 GFP were successfully expressed in mammalian cells and retained part of their fluorescence, making them a new potential bimodal reporter gene.**

The discovery, isolation, cloning, and expression of green fluorescent protein (GFP)<sup>1</sup> has revolutionized the field of reporter genes, allowing scientists to visualize cellular processes in real-time. Since then, directed mutagenesis of GFP has provided us with multi-color fluorescent reporter genes<sup>2</sup>, further expanding the use of GFP for the detection of multiple cell types. However, the limited depth of light penetration for such imaging reporters calls for alternative strategies for imaging reporter gene expression. Recent advances in the field of molecular magnetic resonance imaging (MRI) have increased our ability to monitor gene expression in deep tissue, using various MRI contrast mechanisms<sup>3</sup>. One such example is the Lysine-Rich-Protein (LRP)<sup>3b</sup>, a prototype artificial reporter gene that produces MRI contrast based on the chemical exchange saturation transfer (CEST) mechanism<sup>4</sup>. The positively charged amino acids (mostly lysine and arginine) in peptides and proteins enable their use as CEST-based contrast agents<sup>5</sup> or reporter genes<sup>6</sup>. In an effort to develop alternative CEST reporter genes, with a defined structure and controlled expression level, we investigated whether superpositively charged mutants<sup>7</sup> of GFP could be used as CEST reporter genes, based on their high content of lysine and arginine residues.

*E. coli* optimized genes encoding to wild type (wt) GFP (total charge of -7) and its superpositively charged variants (+36 and +48) were transformed into BL21 chemically competent *E. coli* cells. Recombinant wt and mutated GFP proteins, fused to histidine tags, were expressed and purified using immobilized metal affinity chromatography, followed by dialysis with 10 mM PBS, pH=7.2 containing 2 M NaCl as previously described<sup>7a</sup>. Protein solutions

were concentrated and aliquots were stored at -80°C for further experiments. After evaluation of the protein purification and fluorescence (Fig 1a), the pH of the protein solutions was adjusted to 7.2. CEST experiments were performed using variable levels of saturation power ( $B_1$ ) (Fig. 1). Both +36 GFP and +48 GFP showed a significantly higher CEST contrast compared to wt GFP under all conditions. Fig. 1b demonstrates the MTR asymmetry ( $MTR_{asym}$ ) maps obtained from 1.25 mg/mL pure protein solution at pH=7.2, with the saturation pulse applied at  $\Delta\omega=1.8$  ppm offset from the frequency of the water protons.

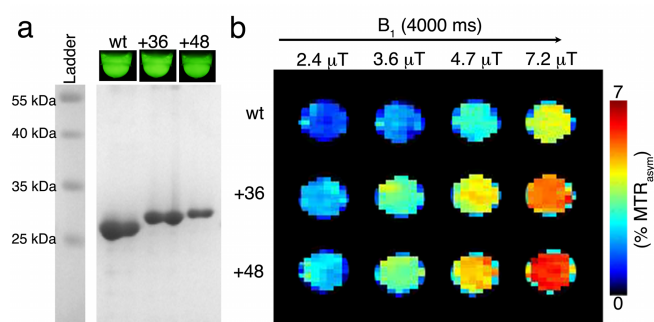


**Figure 1.** CEST MRI of GFP proteins. a) Fluorescence of the examined GFP proteins and their purity, as determined by SDS-polyacrylamide gel electrophoresis. b)  $MTR_{asym}$  maps obtained for a saturation pulse at  $\Delta\omega=1.8$  ppm frequency offset. Shown is the dependency of CEST contrast on  $B_1$  power. CEST data from 1.25 mg/ mL pure protein solutions were acquired at 11.7 T, 37°C, pH=7.2, and  $B_1=4000$  ms.

The  $MTR_{asym}$  plots of the three examined proteins at different  $B_1$  values are shown in Fig. 2. It can be seen that the highest CEST contrast was obtained when the saturation pulse was applied at the frequency offset of the guanidine exchangeable protons of the arginine amino acids, i.e.,  $\Delta\omega=1.8$  ppm. This characteristic  $MTR_{asym}$  signature was previously demonstrated for arginine-rich synthetic

peptides<sup>8</sup> and proteins (either naturally occurring salmon<sup>5a</sup> or human protamine<sup>6</sup>). From Figs. 1 and 2, it is clear that when a stronger B<sub>1</sub> saturation pulse is used, a higher CEST contrast can be obtained for all three GFP proteins. When 7.2  $\mu$ T was used as B<sub>1</sub> saturation pulse, a higher CEST contrast is obtained from +48 GFP compared to +36 GFP. At a lower power (i.e., 3.6  $\mu$ T) the relative CEST effect is much higher between the mutated GFPs (either +48 or +36) and the wt GFP (see Fig. S1, S2 and Table S1, Electronic supporting information). It should be noted that, although strong saturation pulses may increase the CEST contrast, this might also trigger a higher magnetization transfer (MT) effect from biological tissues, which should be processed and filtered properly. In addition, the back-exchange process that reduces the CEST effect is also a major factor at stronger-than-optimal B<sub>1</sub><sup>4</sup>.

Although GFP has been suggested previously as a reporter platform for MRI, based on the magnetization transfer contrast mechanism<sup>9</sup>, our data demonstrate the much higher specificity when using supercharged GFP reporters and CEST instead of MT as the contrast mechanism. The strong CEST peak at the 1.8 ppm frequency offset, which is characteristic for arginine-rich proteins, makes the supercharged GFP mutants unique for MRI applications, with well-characterized imaging features compared to native proteins with a more normal distribution of amino acids.

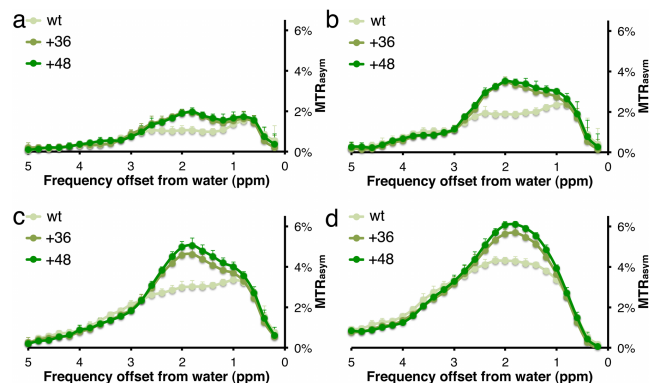


**Figure 2.** MTR<sub>asym</sub> plots of GFP proteins as a function of applied saturation pulse (B<sub>1</sub>) power: a) 2.4  $\mu$ T; b) 3.6  $\mu$ T; c) 4.7  $\mu$ T; and d) 7.2  $\mu$ T. Data from 1.25 mg/mL pure protein solutions were acquired at 11.7 T, 37°C, pH=7.2, and B<sub>1</sub>=4000 ms. N=7 for each sample, error bars represent standard deviation.

Interestingly, no difference in CEST contrast (i.e., MTR<sub>asym</sub> values) could be obtained when the saturation pulse was performed at the frequency offset of the amide protons (i.e.,  $\Delta\omega=3.6$  ppm) for either of the mutants, compared to wt GFP (see Fig. 2). It is known that high CEST contrast from the amide protons of lysine-rich proteins is obtained only where the contributing NH- proton is that of the amide bond between neighbouring positively charged amino acids<sup>10</sup> or in other well-defined amino acid sequences<sup>5a</sup>. Therefore, no CEST contribution was observed from the added lysine amino acids (see Table 1). In addition, the amine exchangeable protons of the lysine side chain are protonated at physiological pH ( $-\text{NH}_3^+$ ) and exchange too fast with water protons in order to be observed in CEST experiments performed at 11.7 T. Therefore, the only amino acids from the mutants contributing to the CEST contrast are the water-exposed additional arginines (see Table 1). Although lysine is two times more abundant in +48 GFP (42 lysine/protein) than in wt GFP (20 lysine/protein), no difference was observed at  $\Delta\omega=3.6$  ppm offset. However, as shown in Figs. 1 and 2 and in Table 1, an

increasing number of arginine residues do, indeed, contribute to higher CEST contrast at 1.8 ppm from both +36 GFP (20 arginine/protein) and +48 GFP (21 arginine/protein). As demonstrated for several other CEST probes, the addition of exchangeable protons does not always increase the obtained CEST contrast<sup>5a,10</sup>. This may be explained by the occurrence of a back exchange from saturated water protons to the CEST probes at higher concentrations. In addition, the exchange rate (and hence CEST contrast) between exchangeable protons from the same functional groups located at different protein positions may alter the CEST contrast. As a result, it is difficult to predict the increase in contrast that could be obtained from additional exchangeable protons, such as from the extra arginines in this study.

Gene optimization is essential for the expression of CEST arginine-rich proteins in bacteria<sup>6,8</sup>. To enable successful reporter gene expression in eukaryotes, the genes encoding for wt, +36, and +48 GFP were optimized to enable the expression in mammalian cells (for optimized gene sequences, see ESI). Human embryonic kidney (HEK) 293T cells were transfected with wt, +36, or +48 GFP mammalian-optimized genes to assess their potential as bimodal reporter genes. All three variants of GFP were expressed in HEK 293 cells 24 hours post transfection (Fig. 3). In addition to wt GFP, both CEST-generating GFP mutants still exhibited cellular fluorescence, albeit lower for +48 compared to +36, a phenomenon that should be further explored. One possible explanation for the observed reduction in cellular fluorescence is that superpositively charged proteins can bind to negatively charged entities such as nucleic acids, which may lead to their aggregation.<sup>7a</sup>

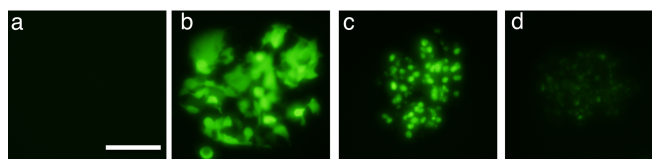


**Figure 3.** Fluorescent microscopy images of human embryonic kidney cells (HEK293T) without transfection (a) and 24 hrs after transfection with optimized genes encoding for b) wt, c) +36, and d) +48. Bar: 100  $\mu$ m.

Other strategies have been suggested for imaging gene expression with CEST MRI<sup>11</sup>, in which improved contrast specificity can be obtained by administering probes that increase the chemical shift offsets of exchangeable protons<sup>12</sup>. However, the necessity of probe administration and sufficient accumulation may be difficult or not possible in certain applications. This includes studying the central nervous system, where the blood brain barrier may prevent the uptake of injected imaging probes. Therefore, imaging reporters that can be directly detected by endogenous expression are, in some cases, most desirable<sup>6,9,13</sup>, including supercharged GFPs.

**Table 1:** Number of positively charged amino acids and their measured MTR<sub>asym</sub> value (1.25 mg/mL; B<sub>1</sub>=4.7  $\mu$ T). N=7 for each sampled protein.

	No. of lysines	MTR <sub>asym</sub> 3.6 ppm	No. of arginines	MTR <sub>asym</sub> 1.8 ppm
wt GFP	20	1.3 $\pm$ 0.1%	7	3.0 $\pm$ 0.3%
+36 GFP	36	1.2 $\pm$ 0.3%	20	4.6 $\pm$ 0.3%
+48 GFP	42	1.2 $\pm$ 0.3%	21	5.1 $\pm$ 0.3%

## Conclusions

Superpositively-charged GFP mutants have potential for use as CEST MRI reporter genes while retaining their optical properties. The replacement of specific amino acids with arginine can increase the CEST signal, while maintaining the protein structure and function. These findings suggest that molecular engineering of existing proteins may be used to create a new generation of molecular probes. Such a bi-modal probe, if furthered optimized as a robust reporter gene system, may allow fluorescent pre-sorting of the cells of interest prior to *in vivo* administration and MRI detection, and may provide intrinsic validation of CEST MRI by post-mortem fluorescence.

## Notes and references

<sup>a</sup> Russell H. Morgan Department of Radiology and Radiological Science, Division of MR Research, the Johns Hopkins University School of Medicine Baltimore, Maryland, USA

<sup>b</sup> Cellular Imaging Section and Vascular Biology Program, Institute for Cell Engineering, the Johns Hopkins University School of Medicine Baltimore, Maryland, USA

<sup>c</sup> Department of Chemical & Biomolecular Engineering, the Johns Hopkins University School of Medicine Baltimore, Maryland, USA

<sup>d</sup> Department of Biomedical Engineering, the Johns Hopkins University School of Medicine Baltimore, Maryland, USA

<sup>e</sup> Department of Oncology, the Johns Hopkins University School of Medicine Baltimore, Maryland, USA

<sup>f</sup> F.M. Kirby Research Center for Functional Brain Imaging, Kennedy Krieger Institute, Baltimore, Maryland, USA

†The study was supported in part by 2 RO1 NS045062, MSCRF-0151-00, and MSCRF-0042. We are grateful to Dr. David R. Liu for providing the supercharged GFP plasmids. Electronic Supplementary Information (ESI) available: Experimental methodologies, mammalian-optimised genes sequences and Figures. See DOI: 10.1039/c000000x/

- 1 M. Chalfie, Y. Tu, G. Euskirchen, W. W. Ward and D. C. Prasher, *Science*, 1994, **263**, 802.
- 2 N. C. Shaner, R. E. Campbell, P. A. Steinbach, B. N. Giepmans, A. E. Palmer and R. Y. Tsien, *Nat Biotech*, 2004, **22**, 1567.
- 3 (a) B. Cohen, K. Ziv, V. Plaks, T. Israely, V. Kalchenko, A. Harmelin, L. E. Benjamin and M. Neeman, *Nat Med*, 2007, **13**, 498; (b) A. A. Gilad, M. T. McMahon, P. Walczak, P. T. Winnard, Jr., V. Raman, H. W. van Laarhoven, C. M. Skoglund, J. W. Bulte and P. C. van Zijl, *Nat Biotech*, 2007, **25**, 217; (c) G. Genove, U. DeMarco, H. Xu, W. F. Goins and E. T. Ahrens, *Nat Med*, 2005, **11**, 450; (d) A. Y. Louie, M. M. Huber, E. T. Ahrens, U. Rothbacher, R. Moats, R. E. Jacobs, S. E. Fraser and T. J. Meade, *Nat Biotech*, 2000, **18**, 321.
- 4 P. C. van Zijl and N. N. Yadav, *Magn Reson Med*, 2011, **65**, 927.
- 5 (a) M. T. McMahon, A. A. Gilad, M. A. DeLiso, S. M. Berman, J. W. Bulte and P. C. van Zijl, *Magn Reson Med*, 2008, **60**, 803; (b) N. Oskolkov, A. Bar-Shir, K. W. Chan, X. Song, P. C. van Zijl, J. W. Bulte, A. A. Gilad and M. T. McMahon, *ACS Macro Lett*, 2015, **4**, 34.

- 6 A. Bar-Shir, G. Liu, K. W. Chan, N. Oskolkov, X. Song, N. N. Yadav, P. Walczak, M. T. McMahon, P. C. van Zijl, J. W. Bulte and A. A. Gilad, *ACS Chem Biol*, 2014, **9**, 134.
- 7 (a) M. S. Lawrence, K. J. Phillips and D. R. Liu, *J Am Chem Soc*, 2007, **129**, 10110; (b) J. J. Cronican, D. B. Thompson, K. T. Beier, B. R. McNaughton, C. L. Cepko and D. R. Liu, *ACS Chem Biol*, 2010, **5**, 747; (c) B. R. McNaughton, J. J. Cronican, D. B. Thompson and D. R. Liu, *Proc Natl Acad Sci USA*, 2009, **106**, 6111.
- 8 R. D. Airan, A. Bar-Shir, G. Liu, G. Pelled, M. T. McMahon, P. C. van Zijl, J. W. Bulte and A. A. Gilad, *Magn Reson Med*, 2012, **68**, 1919.
- 9 C. J. Perez-Torres, C. A. Massaad, S. G. Hilsenbeck, F. Serrano and R. G. Pautler, *NeuroImage*, 2010, **50**, 375.
- 10 N. Goffeney, J. W. Bulte, J. Duyn, L. H. Bryant, Jr. and P. C. van Zijl, *J Am Chem Soc*, 2001, **123**, 8628.
- 11 (a) A. Bar-Shir, G. Liu, Y. Liang, N. N. Yadav, M. T. McMahon, P. Walczak, S. Nimmagadda, M. G. Pomper, K. A. Tallman, M. M. Greenberg, P. C. van Zijl, J. W. Bulte and A. A. Gilad, *J Am Chem Soc*, 2013, **135**, 1617; (b) G. Liu, Y. Liang, A. Bar-Shir, K. W. Chan, C. S. Galpoththawela, S. M. Bernard, T. Tse, N. N. Yadav, P. Walczak, M. T. McMahon, J. W. Bulte, P. C. van Zijl and A. A. Gilad, *J Am Chem Soc*, 2011, **133**, 16326; (c) Y. Jamin, T. R. Eykyn, E. Poon, C. J. Springer and S. P. Robinson, *Molecular Imaging and Biol*, 2014, **16**, 152.
- 12 A. Bar-Shir, G. Liu, M. M. Greenberg, J. W. Bulte and A. A. Gilad, *Nat Protocol*, 2013, **8**, 2380.
- 13 (a) M. H. Vandsburger, M. Radoul, Y. Addadi, S. Mpfu, B. Cohen, R. Eilam and M. Neeman, *Radiology*, 2013, **268**, 790; (b) B. Iordanova and E. T. Ahrens, *NeuroImage*, 2012, **59**, 1004.